



Contents lists available at ScienceDirect

## Materials Today: Proceedings

journal homepage: [www.elsevier.com/locate/matpr](http://www.elsevier.com/locate/matpr)

# Stress relaxation in asymmetric bistable composites: Experiments and simulations

Francesco Nicassio\*, Gennaro Scarselli, Francesca Lionetto, Alfonso Maffezzoli

Department of Engineering for Innovation, University of Salento, Via per Monteroni, Lecce 73100, Italy

## ARTICLE INFO

### Article history:

Received 3 September 2019

Accepted 5 December 2019

Available online xxxx

### Keywords:

Stress relaxation

Asymmetric composite laminates

Bistable plates

Smart materials

Zener model

## ABSTRACT

In the last years, bistable composite structures are finding interest in several aeronautical applications such as power harvesting devices or morphing applications on very small aircraft/drones, not needing servo-activated control systems. Residual stresses, developed upon cooling after curing, leads to warped the composite laminates. Several batches of unsymmetrical and unbalanced  $[0^\circ/90^\circ]$  laminates were cured in an autoclave according to a standard temperature cycle, following the pre-preg supplier suggested curing cycle. In order to increase the thermal stresses (and hence the bistability phenomenon), these laminates were removed from the autoclave immediately after the curing reaction and rapidly cooled down at room temperature not applying the indicated cool rate between 2 and  $5^\circ\text{C min}^{-1}$ . During storage at room temperature, thermal stresses changed over time, indicating that asymptotic stress relaxation occurs. The first part of this work looks at residual stress characterization of bistable composite plates measuring the changes of shape observed during room temperature annealing. Rectangular plates were produced and the bistable geometric shapes were accurately assessed using a laser scanner system over several days, in order to monitor the curvature changes due to stress relaxation. Then phenomenological viscoelastic predicting models were proposed for a quick estimate for the strain/stress relaxation phenomenon. The loss of bistability was demonstrated with the help of numerical simulation and experimental testing. The final goal was to gain a better knowledge of the relation between processing and final shape of bistable laminates, in order to make them suitable for application on small air vehicles.

© 2019 Elsevier Ltd. All rights reserved.

Selection and peer-review under responsibility of the scientific committee of the 12th International Conference on Composite Science and Technology.

## 1. Introduction

In recent years, the nonlinear behavior of thin asymmetric composite laminates inspired researchers to explore bistable structures that can be used for morphing and energy harvesting. The bistability phenomenon of a structure is the property of possessing two stable equilibria, each of which is an equilibrium position [1–3]. Therefore, the structure can settle at either of them without demanding an external load: asymmetric  $[0^\circ/90^\circ]$  composite laminates exhibit mechanical bistability that enables them to assume large deflections from one equilibrium position to another with only small energy input (ideal for morphing structures [4–7] and power harvesting systems [8–11]).

The final room-temperature shapes of composites laminates depend on the laminate size, thickness, layout and cure temperature. The bistability of a composite laminate occurs due to residual stresses, generated during rapid cooling down at room temperature, resulting from differences in coefficients of thermal expansion and elastic properties for each lamina [12]. So during the manufacturing process of these composite laminates, the residual thermal stresses play a key role in their bistable behavior; the latter was analyzed by a number of authors. In [13] sensitivity analysis was performed on analytical models of bistable composite laminates to establish the influence of material, geometric and environmental uncertainties on laminate curvatures. The results reveal significant sensitivities of the laminate to Young's moduli  $E$ , the transverse thermal expansion coefficients, ply thickness and the temperature change from cure. Brampton et al. [13] concluded that significant improvements in the accuracy of bistable laminate shape predictions can be achieved if the laminate mate-

\* Corresponding author.

E-mail address: [francesco.nicassio@unisalento.it](mailto:francesco.nicassio@unisalento.it) (F. Nicassio).

rial properties, structure and operating environment are accurately characterized. The main purpose of Moore in [14] was to investigate the effect of the temperature dependency of material properties on the cured shapes of graphite-epoxy composite laminate with different stacking sequence. Furthermore the effect of the resin layers thickness on the actuation loads that triggers the snap-through and snap-back phenomena were also studied.

Despite the bistable composite laminates have received a great deal of research work due to their promising performance, a limited number of scientific literature sources took into account a strain-stress models of bistable composite laminates including time dependent effects. Cho et al. [15] presented a theoretical analysis and experiments on the room-temperature curvature shapes of unsymmetric laminates, including relaxation effect. From this analysis, the processing parameters influencing the final cured shape of laminates were globally investigated by quantitative prediction of relaxation coefficients. By experimentally identifying relationships between slippage coefficients and measured curvature values, a parametric study and general simulations were carried out. The curvature of fully cured unsymmetric  $[0^\circ/90^\circ]$  laminates was measured and analyzed by Wijskamp et al. in [16]. This curvature was demonstrated to be a good measure for the transverse stress being present in the  $90^\circ$  ply before the laminate is released from the tool. Firstly, the transverse stress was predicted using an analytical, linear elastic approach including thermal shrinkage and contraction of the resin due to crosslinking. Secondly, the residual stress state before release from the tool was calculated numerically applying a viscoelastic material model. The model incorporated the cure conversion and the resulting change in viscosity, both fitted on experimentally obtained data. Cowley and Beaumont in [17] carried out measurements of the residual stress in a thermoplastic matrix and a toughened thermosetting matrix, both reinforced with carbon fiber. Stress relaxation effects at  $20^\circ\text{C}$  were measured by recording the curvature of unsymmetrical specimens over 5000 h: stress relaxation occurred at room temperature and residual stresses can decrease by up to 25%. The effect of cooling rate from the molten state and annealing from the amorphous state on residual stress development in graphite fiber reinforced polyetheretherketone laminates was experimentally studied by Unger and Hansen in [18]. The degree of stress relaxation occurring during the cooling cycle was studied by measuring curvature change of nominally processed specimens as a function of time and temperature. It was found that most stress relaxation occurred in the vicinity of the glass transition temperature  $T_g$ : the curvature changed of only 18.8% for a dwell time of 146 min. At temperatures above and below  $T_g$ , stress relaxation effects were found to be negligible.

In this work the dynamical characterization of time dependent stress in bistable composite plates, due to curing cycle and cooling down during manufacturing process is presented. Several bistable

plates were fabricated and cured in autoclave; the main stress relaxation effect was monitored by measuring the maximum chamber of each stable state by laser scanner acquisitions of bistable plate shapes. The assumption of intralaminar transverse relaxation or interlaminar shear relaxation were tested. Analytical and Finite Elements (FE) models were adopted in order to simulate and better understand the physical mechanism underlying the stress relaxation in the mentioned bistable composite laminates. The analysis, validation and experimentation processes are sketched in Fig. 1: the dotted double arrow lines indicate the correlation between experimental and analytical or numerical results.

## 2. Materials

Asymmetrical  $[0^\circ/90^\circ]$  laminates were fabricated laying up 2 unidirectional prepreg plies made of IM7 carbon fiber and 8552 epoxy matrix (HexPly<sup>®</sup>8552 from Excel). Prepreg mechanical and physical properties are shown in Table 1.

Three identical batches of two rectangular plates (see Fig. 2) with aspect ratio (AR) of 2 (80 mm  $\times$  160 mm) were manufactured.

The rectangular shape of the laminates was chosen in order to enhance the asymmetry between the  $0^\circ$  and  $90^\circ$  oriented plies, thus increasing the maximum curvature after curing and cooling to room temperature. Samples were cured in autoclave using the recommended cure cycle (shown in Fig. 3) for the HexPly<sup>®</sup> 8552 prepreg.

In order to increase the thermal residual stresses and to obtain a higher level of curvature in the samples, each batch was removed from the autoclave immediately after the curing reaction and rapidly cooled down in open air (dotted line in Fig. 3) not adopting the recommended cool rate of  $2\text{--}5^\circ\text{C}/\text{min}$ , i.e. the continuous line in Fig. 3. Upon cooling to room-temperature, each laminate was observed to have the two expected stable states.

Moreover, stress-relaxation tests were performed on 16 plies unidirectional laminate from Hexply<sup>®</sup>8552 prepreg, cured as suggested by the manufacturer.

**Table 1**  
Physical properties of HexPly<sup>®</sup>8552 unidirectional prepreg.

Properties	Units	Values
Nominal cured ply thickness	mm	0.131
Nominal laminate density	$\text{g}/\text{cm}^3$	1.57
$0^\circ$ Tensile Modulus	GPa	164
$90^\circ$ Tensile Modulus	GPa	12
Poisson's Ratio	-	0.316
$0^\circ$ Coefficient of thermal expansion	$1/\text{K}$	$-0.1\text{E-}6$
$90^\circ$ Coefficient of thermal expansion	$1/\text{K}$	$31\text{E-}6$

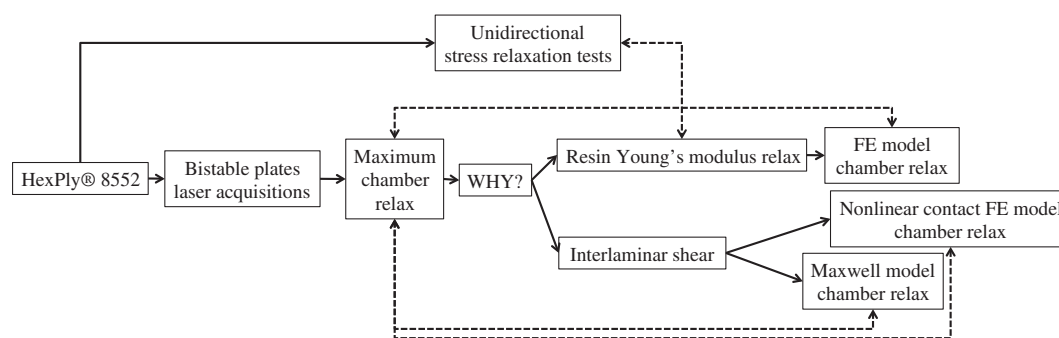


**Fig. 1.** Schematic of the present research.

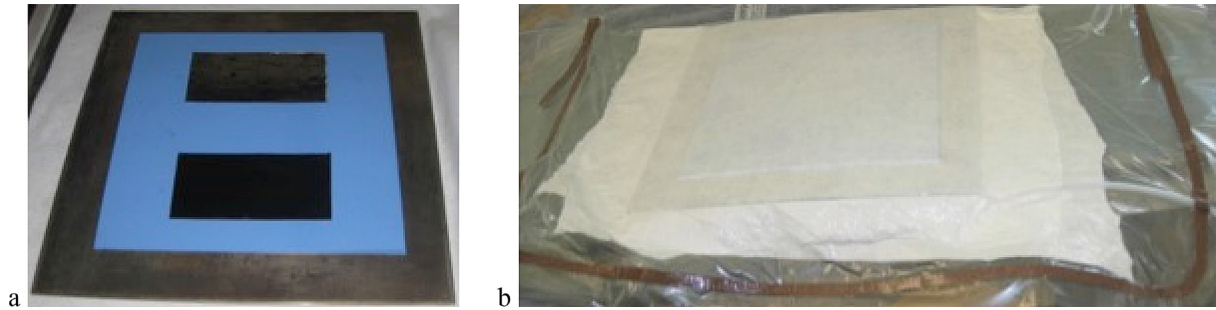


Fig. 2. (a) Batch of two composite laminates; (b) vacuum bag.

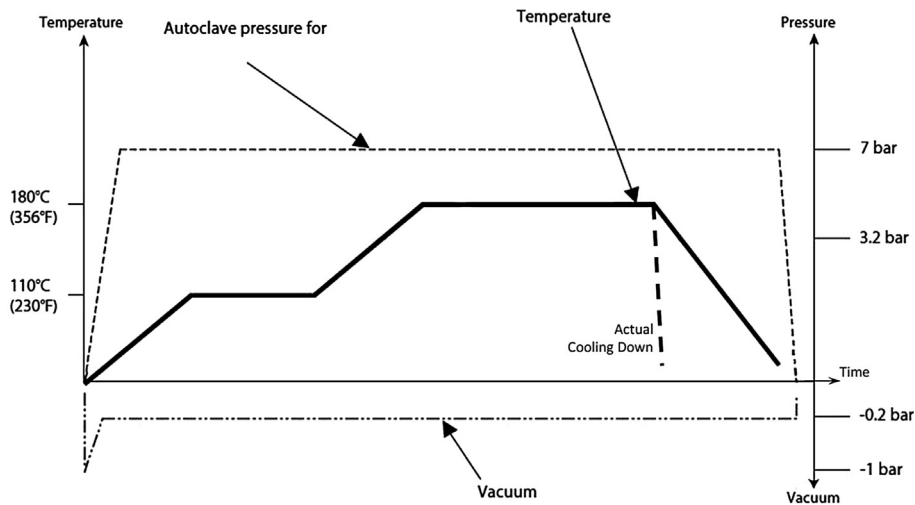


Fig. 3. Recommended cure cycle (continuous line) and actual cooling down (dotted line) for HexPly®8552 unidirectional prepreg.

### 3. Experimental set-up

A dynamometer LLOYD LR50K (Fig. 4(a)), equipped with a load cell of 50 kN and an oven to keep the specimens at constant temperature between curing and room temperature, was used. Strains were measured by a strain gauge.

The cured shapes of the bistable plates were measured using a laser scanner Shape Grabber LM600 (Fig. 4(b)). The laminate surfaces were measured with a resolution of 0.1 mm over the measurement range, performing for each shape five scans for the measurement repeatability.

An \*.STL data file, containing the point clouds coordinates of surfaces, was obtained by Shape Grabber SGCentral software. The maximum chamber was obtained from longitudinal and transversal cross-section by MeshLab software. The maximum chamber reached a constant plateau value in 10 days.

### 4. FE and analytical models

#### 4.1. FE model

The FE model, developed in ANSYS Workbench environment for the two stable shapes shown in Fig. 5, was used (i) to numerically determine the plate shape due to the cooling down from curing temperature and (ii) to simulate the stress relaxation as possible cause leading to chamber decrease during storage at room temperature either using a time dependent modulus  $E_2$  either adopting a friction coefficient between the two laminae, so assuming an interlaminar shear stress relaxation mechanism.

In the case of  $E_2$  modulus relaxation, only one geometrical surface was drawn and the “Layered Section” option was implemented to simulate  $[0^\circ/90^\circ]$  stacking sequence. While, when an interlaminar shear relaxation mechanism was assumed, two distinct facing surfaces were necessarily meshed (with  $0^\circ$  and  $90^\circ$  orientations, respectively) to allow the two contacting geometries to carry shear stresses up to a certain magnitude across their interface before they start sliding. The option “Large Deflection” was employed because of large deformation of the studied laminates. The temperature profile, applied to the mesh nodes to simulate the cooling down process, was a linear ramp in the transient analysis from 180 °C to 20 °C in 60 s. The final relaxed shapes were achieved by splitting up the numerical nonlinear analysis in two load cases: first step with the thermal load, assuming a linear elastic behavior of composite, and second step (10 days equal to 864,000 s) with time dependent material properties in order to simulate transversal  $E_2$  modulus relaxation or the activation of “Frictional Status” between the two surfaces to simulate the interlaminar shear effect. In particular as a consequence of the high deformation gradients (fast increases of deformation of the laminate during cooling) the minimum time step was set at 1e-3 s, whilst for low deformation gradients (slow decreases of deformation of the plate during the relaxation at room temperature) the minimum time step was 36 s. In this way, the convergence is guaranteed for each time step.

#### 4.2. Analytical Zener model

The bistable plate, when deformed by a thermal load, can be idealized as mass – spring – damper system (Fig. 6a)): the system



Fig. 4. (a) LLOYD Instruments LR50K Plus materials testing machine equipped with oven; (b) ShapeGrabber LM600 3D scanner Batch of two composite laminates.

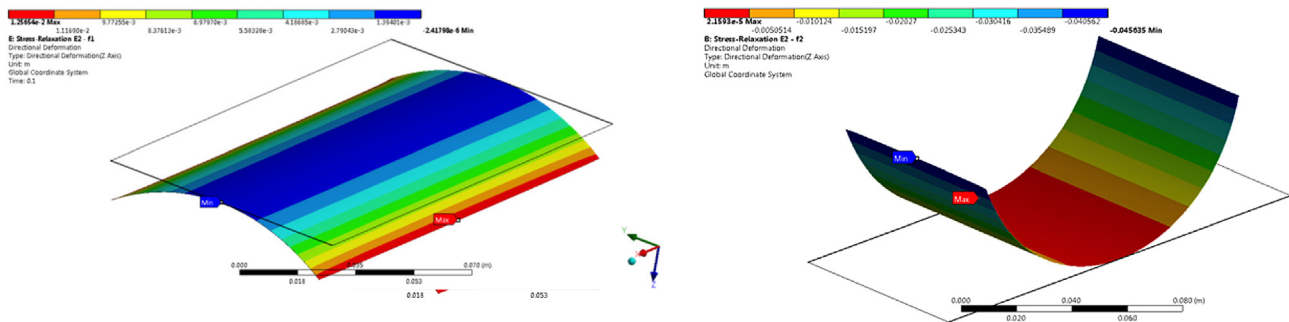


Fig. 5. FE stable shapes (the contour plot provides minimum values, in blue, and maximum values, in red, of nodal displacements). (For interpretation of the references to colour in this figure legend, the reader is referred to the web version of this article.)

(with mass  $m$  equal to the actual plate mass, stiffness  $k$  and damping  $c$  in Fig. 6(a)) represents the entire bistable plate. More complex systems could provide a better approximation of the actual laminate, but this two degrees of freedom model (characterized by vertical displacements  $x_1$  and  $x_2$ ) can provide a phenomenological interpretation of the observed relaxation behavior. The mechanical model is the standard linear solid model, Zener model in Kelvin representation, and it consists of two springs (for the sake of simplicity assumed with equal stiffness) and a damper.

By using the free body diagrams in Fig. 6(b) and (c), the motion equation of the bistable Zener model can be stated as:

$$\begin{cases} m\ddot{x}_1 + k(x_1 - x_2) = 0 \\ 0\ddot{x}_2 + c\dot{x}_2 + kx_2 - k(x_1 - x_2) = 0 \end{cases} \quad (1)$$

where  $x_1$  is the vertical displacement of the main system, corresponding to the actual maximum chamber of the bistable plate and  $x_2$  is a fictitious point.

It is noteworthy that Eq. (1) represents an unforced damped system: it was solved with initial boundary conditions equal to the actual maximum chambers (one per stable state) due to the cooling down process. The aim of this analytical model is to simulate the exponential decay of these chambers, by using  $k$  and  $c$  coefficients as “fudge factors” in order to fit the experimental results.

5. Results

The maximum plate chambers in both stable states were measured via laser acquisition immediately after cooling and until the 9th day.

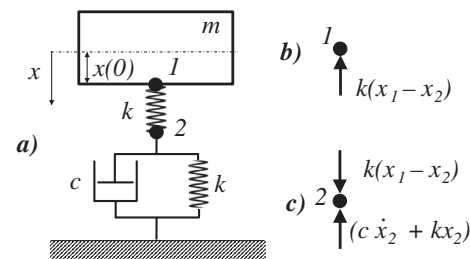


Fig. 6. (a) Bistable plate mechanical model; (b) and (c) free body diagram of point 1 and 2.

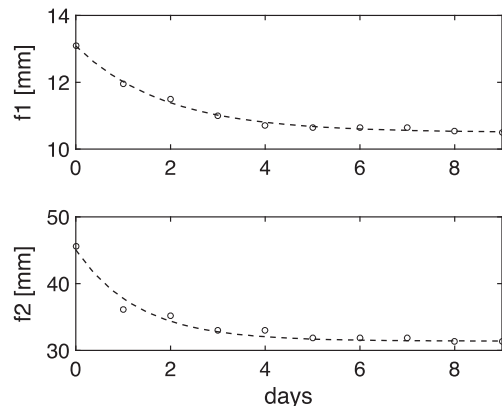
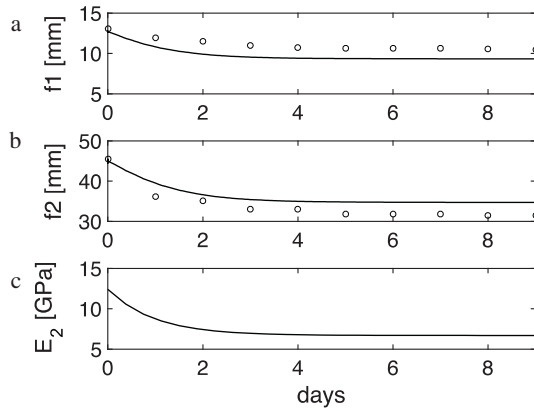
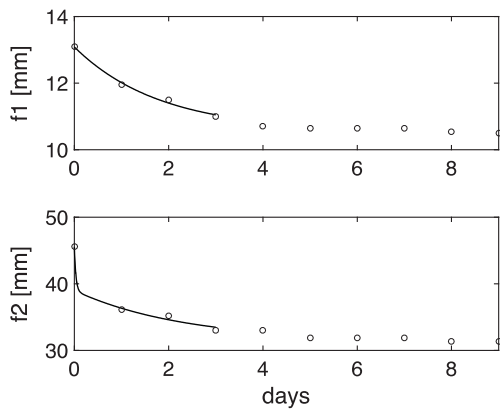


Fig. 7. Actual maximum chamber time evolution (scatter plot) and relative exponential fitting (dotted line).



**Fig. 8.** Comparison between experimental values (scatter plot) and FE maximum bistable chamber evolution (a) and (b) due to resin modulus relaxation (c).



**Fig. 9.** Comparison between experimental values (scatter plot) and FE maximum bistable chamber evolution due to interlaminar shear.

As shown in Fig. 7, a clear exponential trend in the measurements can be observed. The decay curves  $f_{1/2}(t)$  for each stable state can be fitted by:

$$f_{1/2}(t) = f_{1/2}(0)e^{-\frac{t}{\tau_{1/2}}} \quad (2)$$

where  $f_{1/2}(0)$  is the maximum chambers for each stable state due to the cooling down process, while  $\tau_{1/2}$  is the relaxation time of each stable shape at which the chamber is reduced to  $1/e$  times its initial value. The different relaxation behavior of the chambers of investigated plates was clearly identified in Fig. 7: the smaller chamber,

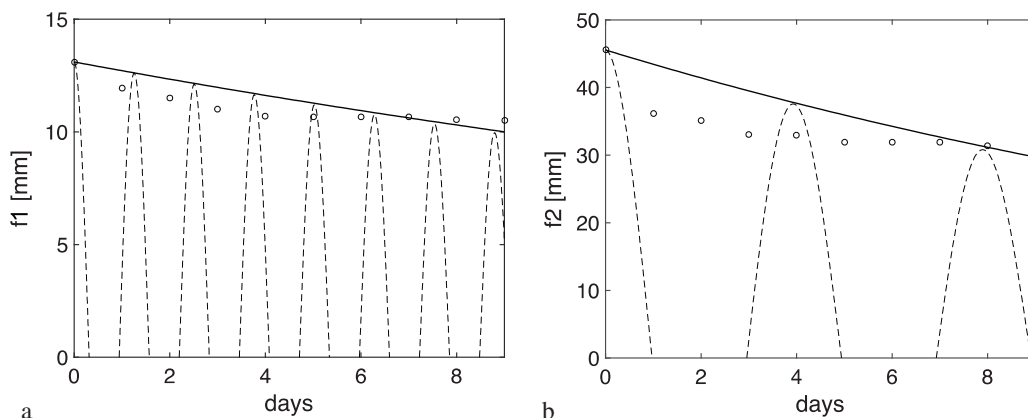


**Fig. 10.** Comparison between experimental values (scatter plot) and exponential decay of the Zener model (continuous line): (a)  $f_1$ ; (b)  $f_2$ .

measured along the laminate width, relaxed ( $-20\%$  after 9 days) less than the bigger one ( $-31\%$  after 9 days), measured along the laminate length.

At first, the relaxation of  $E_2$  modulus of each lamina considered responsible of this behavior.

Fig. 8(c) shows  $E_2$  modulus evolution needed in FE simulations to fit the chamber change at room temperature (Fig. 8(a) and (b)). The isothermal stress relaxation experiments showed that  $E_2$  only relaxed for 5% of initial post curing value (instead of 41% needed in FE simulations).

This suggest that the intralaminar relaxation cannot be considered responsible of the chamber reduction measured at room temperature.

Excluding that relaxation can occur in fiber direction, the interlaminar shear was assumed as mechanism leading to bistable relaxation. In this FE scenario, the two contacting surfaces started sliding relative to each other after the cooling down step. The frictional model automatically defined an equivalent shear stress at which sliding on the geometry began as a fraction of the contact pressure. Once the shear stress was exceeded, the two geometries slid relative to each other because of thermal residual stress in each lamina. The coefficient of friction, equal to 0.998, provided the results plotted in Fig. 9: because of the long time required for contact computation, the evolution of the maximum chambers was simulated only for 3 days after the cooling down. A good correlation between this FE model results and experimental data is observed.

In order to overcome the long FE computational time, the phenomenological standard linear solid model shown in Fig. 6 was developed. The boundary conditions were perturbed by the initial maximum chamber values and the underdamped solutions of Zener model is reported in Fig. 10 (dotted line) with the decay envelope describing how the oscillation decays exponentially. Different pattern of relaxed chamber (analytical trend in continuous line vs experimental data in circle) indicated that the used analytical model is too simple and  $k$  and  $c$  factors are insufficient to describe correctly the relaxation of the bistable plate.

In the light of the results of the presented study, the targets of future works will be to:

- investigate the interlaminar shear, by means of a double-notch shear test with IM7/8552 specimens in order to measure interlaminar shear relaxation;
- upgrade the computing power to carry out increasingly complex FE simulation;
- develop a generalized analytical model (combining more spring-dashpot elements) in order to accurately reflect the relaxation behavior of bistable plates.

## 6. Conclusions

In this paper the bistable composite plate behavior in terms of stress relaxation was studied, using experimental data, FE and analytical simulations. The main target of this work was to investigate the key element of this phenomenon: the interlaminar shear among the laminas. The experimental campaign provided many information about the relaxation in terms of the maximum chamber reduction of the two stable states. Only the frictional FE model gave good numerical/experimental correlations, whereas the resin relaxation simulations and the Zener model behavior demonstrated the inconsistency of the used decay resin properties and the inadequacy of the simple analytical model, in terms of maximum chambers evolution and time relaxation. The investigation of the bistable features after cooling down process was needed to define the starting point for the next goal: dynamical models of bistables, with stack sequences optimized through Genetic Algorithms [19], including interlaminar shear time dependent effects.

## Acknowledgements

The authors wish to thanks Giuseppe Buccoliero and Clara Pezuto for the support to sample fabrication and stress relaxation measurements, respectively. Adriana Bandiera and Dario De Pascali (SIBA, University of Salento) are kindly acknowledged for the use of laser scanner. This work was also supported by Italian Minister for University and Research through the PON research project MAIPCO.

## References

- [1] R.L. Harne, K.W. Wang, A review of the recent research on vibration energy harvesting via bistable systems 023001 *Smart Mater. Struct.* 22 (2013), <https://doi.org/10.1088/0964-1726/22/2/023001>.
- [2] S.A. Emam, D.J. Inman, A review on bistable composite laminates for morphing and energy harvesting 060803 *Appl. Mech. Rev.* 67 (2015), <https://doi.org/10.1115/1.4032037>.
- [3] X. Lachenal, S. Daynes, P.M. Weaver, Review of morphing concepts and materials for wind turbine blade applications, *Wind Energy* 16 (2013) 283–307, <https://doi.org/10.1002/we.531>.
- [4] F. Nicassio, G. Scarselli, F. Pinto, F. Ciampa, O. Iervolino, M. Meo, Low energy actuation technique of bistable composites for aircraft morphing, *Aerosp. Sci. Technol.* 75 (2018) 35–46, <https://doi.org/10.1016/j.ast.2017.12.040>.
- [5] A.J. Lee, A. Moosavian, D.J. Inman, A piezoelectrically generated bistable laminate for morphing, *Mater. Lett.* 190 (2017) 123–126, <https://doi.org/10.1016/j.matlet.2017.01.005>.
- [6] F. Nicassio, G. Scarselli, G. Avanzini, G. Del Core, Numerical and experimental study of bistable plates for morphing structures, *Act. Passiv. Smart Struct. Integr. Syst.* 2017 (2017) 101640K, <https://doi.org/10.1117/12.2260099>.
- [7] B. Wang, K.S. Fancey, A bistable morphing composite using viscoelastically generated prestress, *Mater. Lett.* 158 (2015) 108–110, <https://doi.org/10.1016/j.matlet.2015.05.129>.
- [8] G. Scarselli, F. Nicassio, F. Pinto, F. Ciampa, O. Iervolino, M. Meo, A novel bistable energy harvesting concept, *Smart Mater. Struct.* 25 (2016), <https://doi.org/10.1088/0964-1726/25/5/055001>.
- [9] C. Lan, W. Qin, Enhancing ability of harvesting energy from random vibration by decreasing the potential barrier of bistable harvester, *Mech. Syst. Signal Process.* 85 (2017) 71–81, <https://doi.org/10.1016/j.ymssp.2016.07.047>.
- [10] A. Syta, C.R. Bowen, H.A. Kim, A. Rysak, G. Litak, Experimental analysis of the dynamical response of energy harvesting devices based on bistable laminated plates, *Meccanica* 50 (2015) 1961–1970, <https://doi.org/10.1007/s11012-015-0140-1>.
- [11] M. Hwang, A.F. Arrieta, Input-independent energy harvesting in bistable lattices from transition waves, *Sci. Rep.* 8 (2018) 3630, <https://doi.org/10.1038/s41598-018-22003-7>.
- [12] M.-L. Dano, M.W. Hyer, Snap-through of unsymmetric fiber-reinforced composite laminates, *Int. J. Solids Struct.* 39 (2002) 175–198, [https://doi.org/10.1016/S0020-7683\(01\)00074-9](https://doi.org/10.1016/S0020-7683(01)00074-9).
- [13] C.J. Brampton, D.N. Betts, C.R. Bowen, H.A. Kim, Sensitivity of bistable laminates to uncertainties in material properties, geometry and environmental conditions, *Compos. Struct.* 102 (2013) 276–286, <https://doi.org/10.1016/j.compstruct.2013.03.005>.
- [14] M. Moore, S. Ziaei-Rad, H. Salehi, Thermal response and stability characteristics of bistable composite laminates by considering temperature dependent material properties and resin layers, *Appl. Compos. Mater.* 20 (2013) 87–106, <https://doi.org/10.1007/s10443-012-9255-x>.
- [15] M. Cho, M.H. Kim, H.S. Choi, C.H. Chung, K.J. Ahn, Y.S. Eom, A study on the room-temperature curvature shapes of unsymmetric laminates including slippage effects, *J. Compos. Mater.* 32 (1998) 460–482, <https://doi.org/10.1177/002199839803200503>.
- [16] S. Wijskamp, R. Akkerman, E.A.D. Lamers, Residual stresses in non-symmetrical carbon/epoxy laminates, *ICCM-14*, San Diego, USA, 2003.
- [17] K.D. Cowley, P.W.R. Beaumont, The measurement and prediction of residual stresses in carbon-fibre/polymer composites, *Compos. Sci. Technol.* 57 (1997) 1445–1455, [https://doi.org/10.1016/S0266-3538\(97\)00048-1](https://doi.org/10.1016/S0266-3538(97)00048-1).
- [18] W.J. Unger, J.S. Hansen, The effect of cooling rate and annealing on residual stress development in graphite fibre reinforced PEEK laminates, *J. Compos. Mater.* 27 (1993) 108–137, <https://doi.org/10.1177/002199839302700201>.
- [19] G. Scarselli, L. Lecce, Genetic algorithms for the evaluation of the mistune effects on turbomachine bladed disks, in: *ETC 2005 – 6th Conf, Turbomach. Fluid Dyn. Thermodyn.* (2005).